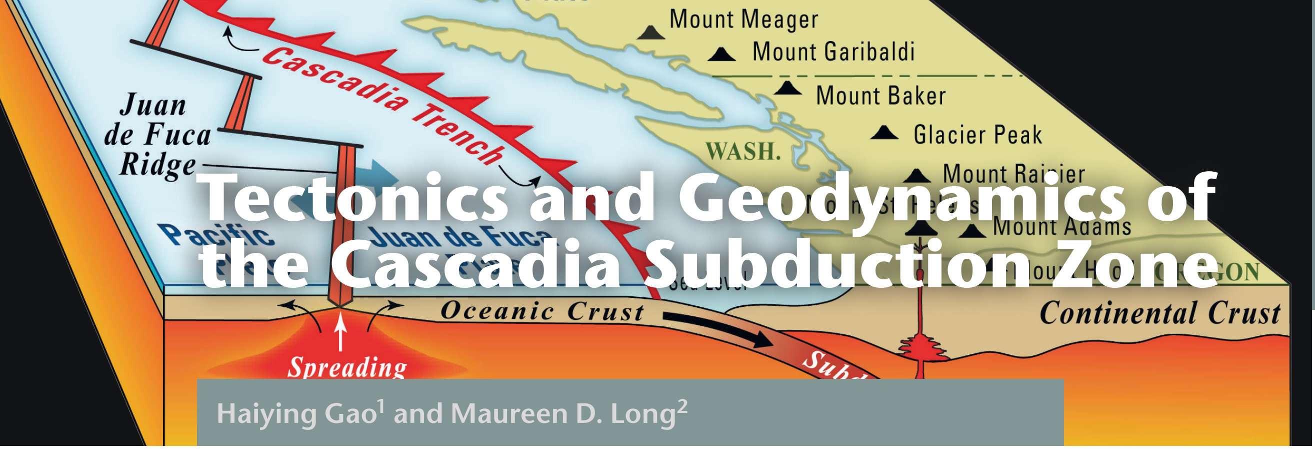

Tectonics and Geodynamics of the Cascadia Subduction Zone

Haiying Gao[1] and Maureen D. Long[2]

1811-5209/22/0018-0226$2.50 DOI: 10.2138/gselements.18.4.226

The Cascadia subduction zone, where the young and thin oceanic Juan de Fuca plate sinks beneath western North America, represents a thermally hot endmember of global subduction systems. Cascadia exhibits complex and three-dimensional heterogeneities including variable coupling between the overriding and downgoing plates, the amount of water carried within and released by the oceanic plate, flow patterns within the mantle wedge and backarc, and the continuity and depth extent of the subducting slab. While recent research has benefitted from extensive onshore and offshore deployments of geophysical instrumentation, a consensus on many important aspects of Cascadia's magmatic, tectonic, and geodynamic setting remains elusive.

Keywords: Cascadia subduction zone; oceanic plate; slab; magmatism; volcano; tectonics

INTRODUCTION

Subduction zones are linear belts on Earth where tectonic plates converge, with one plate sinking into the mantle beneath the other plate, and where the largest earthquakes and volcanoes tend to occur. The Cascadia subduction zone involves the northeastward subduction of the oceanic Juan de Fuca (JdF) plate beneath western North America at a convergence rate of ~3–4.5 cm/y along the trench (Fig. 1). The JdF plate is relatively young (less than 10 million years old), small (only a few hundred kilometers wide from the spreading center to the trench), and thus warm, making Cascadia a hot endmember among subduction zones worldwide. Subduction of the JdF plate results in the ~1300-km-long active Cascade volcanic arc, which extends from northern California through Oregon and Washington, USA, to northern Vancouver Island, Canada (Fig. 1). Arc volcanism initiated ~40 million years ago (Ma), following a change from a previous flat slab configuration, and the most recent event was the major volcanic eruption of Mount St. Helens in 1980. While no large megathrust earthquakes (with magnitudes of ~8–9) have been recorded during the era of modern geophysical instrumentation, paleoseismic studies have demonstrated that Cascadia has hosted megathrust earthquakes in the past, with the most recent event occurring in 1700. With a likely recurrence interval of megathrust earthquakes of ~300–500 years, Cascadia thus faces the threat of potential megathrust earthquakes and associated tsunamis in the near future. The combination of significant risk from geologic hazards and Cascadia's status as an "endmember" among subduction zones worldwide suggests that a thorough understanding of Cascadia's tectonic and geodynamic setting is critically important.

ESTABLISHMENT OF THE MODERN CASCADIA SUBDUCTION SYSTEM

The young JdF plate is a remnant of the old Farallon plate, which has been subducting beneath North America for the last ~180 million years (My). Most of the Farallon slab is understood to have already sunk deep into the mantle beneath North America. Subducted slabs are commonly imaged as high-velocity features by seismic tomography, a method that is analogous to a medical computerized tomography scan but uses seismic waves travelling through the interior of the Earth rather than X-rays. Many seismic tomographic studies have imaged significant high-velocity anomalies in the relatively deep mantle (between ~300 and 1200 km) beneath the central and eastern U.S.; these anomalies are commonly interpreted as remnants of the subducted Farallon slab (e.g., Schmandt and Lin 2014).

Another possible piece of the Farallon slab is the Siletzia oceanic terrane, which accreted onto North America ~45–50 Ma. To the west of the Cascade volcanic arc, the distribution of Siletzia (Fig. 1) is well defined based on geologic outcrops, magnetic and gravity patterns, and seismic images. To the east of the Cascade arc, Siletzia is not exposed, and inferences concerning its distribution and structure are based on indirect evidence and somewhat speculative. Specifically, the southwest–northeast trending Klamath-Blue Mountain lineament in central–north Oregon is proposed to represent a suture between Siletzia and older North America; this is supported by the strong gravity gradient and sharp seismic velocity contrast across the lineament. Gao et al. (2011) suggested that Siletzia is extensively distributed beneath Washington State to the east of the Cascade arc, as inferred from the distribution of high-velocity anomalies within the continental crust (Fig. 1). Schmandt and Humphreys (2011) imaged a large high-velocity column within the upper mantle beneath central Idaho and northern Washington and interpreted it as a remnant of Siletzia oceanic lithosphere. It has been suggested that the accretion of Siletzia onto western North America ended the flat subduction of the Farallon slab and played a critical role in initiating modern Cascadia subduction (e.g., Schmandt and Humphreys 2011).

1 Department of Geosciences
University of Massachusetts Amherst
627 North Pleasant St.
Amherst, MA 01003, USA
E-mail: haiyinggao@umass.edu

2 Department of Earth and Planetary Sciences
Yale University
210 Whitney Avenue
New Haven, CT 06520, USA
E-mail: maureen.long@yale.edu

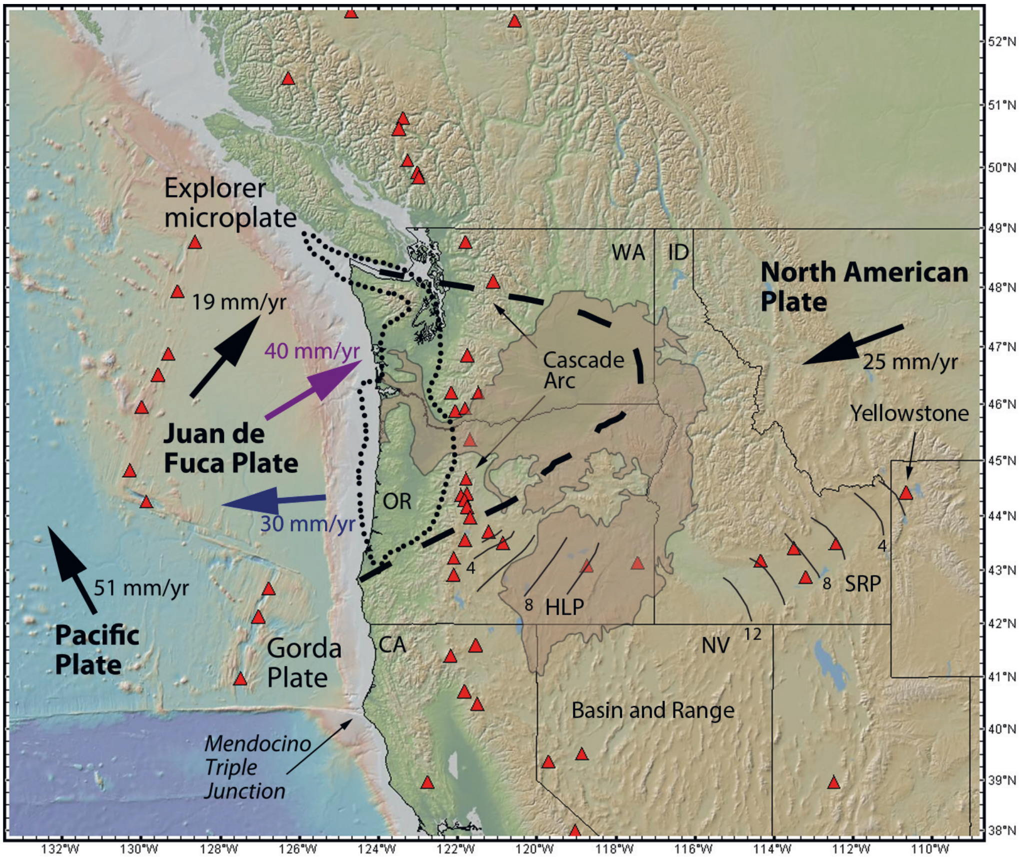

FIGURE 1 Tectonic setting and volcanic features of the Cascadia subduction system. MODIFIED AFTER LONG (2016). The red triangles represent major Holocene volcanoes. Black contours indicate the approximate age progression (in 2-My intervals) of volcanism across the High Lava Plains (HLP) and the Snake River Plain (SRP). The brown area indicates the coverage of the Steens/Columbia River flood basalts. The black dotted line marks the outline of Siletzia west of the Cascades, and the heavy black dashes indicate the inferred outline of Siletzia by Gao et al. (2011). The thick black arrows show absolute plate motions in the hotspot reference frame, the thick purple arrow shows the convergence between the Juan de Fuca and North American plates, and the thick blue arrow shows the rollback of the trench. Details of the underlying data are given in Long (2016) and Gao et al. (2011). CA: California; OR: Oregon; WA: Washington State; ID: Idaho, NV: Nevada.

KEY FEATURES OF THE CASCADIA SUBDUCTION SYSTEM

Among global subduction systems, Cascadia is one of the best instrumented and best studied, with extensive geophysical (and other) data collection. Recent data collection efforts have been enabled by the continent-scale EarthScope USArray and Plate Boundary Observatory, the Cascadia Initiative Community Experiment across the entire oceanic plate, many regional-scale geophysical networks on the continental side, and several active-source seismic experiments within the JdF plate. The excellent data coverage of the entire subduction system from the spreading center to the Cascade arc and backarc makes it feasible to image the entire JdF plate from formation to destruction with seismological (and other) methods. The major structures within the Cascadia subduction system, including the overriding plate, mantle wedge, downgoing plate and its underlying asthenosphere, and backarc mantle, have become much better resolved. A wealth of studies has significantly contributed to our understanding of the structure and dynamics of Cascadia and its context within the global population of subduction zones. Below, we summarize some recent observations along with proposed interpretations in terms of the tectonic evolution in Cascadia.

Geometry of the Oceanic Plate from Formation to Subduction

Oceanic lithosphere is newly formed at spreading centers and becomes older and thicker as it cools and moves toward the trench where the plate bends and subducts. The characteristics of the oceanic plate play a critical role in controlling subduction dynamics, mantle flow patterns, surface magmatism/volcanism, and seismicity. Recent geophysical models of the Cascadia subduction system provide tight constraints on the geometry of the JdF plate from formation to subduction. Prior to subduction, the thickness of the JdF plate is estimated to be less than 40 km based on seismic tomographic images (Gao 2018), consistent with the predicted thickness for a young oceanic plate with a simple cooling model. Near the trench, the seismic velocity of the slab appears to be relatively lower compared with the velocity at other portions of the slab, indicating a presumably weaker segment. One possibility is that the oceanic plate is hydrated near the trench and that bending-related hydration significantly lowers the plate strength. Large-scale, low-velocity anomalies are imaged in the asthenospheric mantle beneath the slab near the trench (Hawley et al. 2016; Bodmer et al. 2020); these anomalies likely require the presence of partial melts, fluids, and/or volatiles. It is possible that the presence of partial melts, fluids, and/or volatiles beneath the slab may play a role in further weakening the slab near the trench.

After subduction at the trench, the JdF plate is clearly imaged as an eastward-dipping, high-velocity feature within the upper mantle of the western U.S. (FIGS. 2 and 3). However, the continuity and depth extent of the subducting slab remain debated. Some studies argue for a continuous slab down to the mantle transition zone at depths of 410–660 km (e.g., Roth et al. 2008), while others have demonstrated that the subducting slab may be fragmented both along the trench direction and along the subduction direction (e.g., Schmandt and Lin 2014; Gao 2018). For example, seismic tomographic models detect two possible gaps in the slab along the trench direction at a depth range of ~75–150 km; one gap is roughly across the California–Oregon state boundary and the other is roughly across the Oregon–Washington state boundary (FIG. 3). The presence of possible slab gaps has also been suggested by analyses of geochemical signatures along the Cascade arc volcanoes (e.g., Mullen et al. 2017). At depths greater than ~150 km, the southern and northern portions of the subducting slab are imaged as continuous high-velocity features, while the slab signature of the central portion appears to be less clear in tomographic models (FIG. 2).

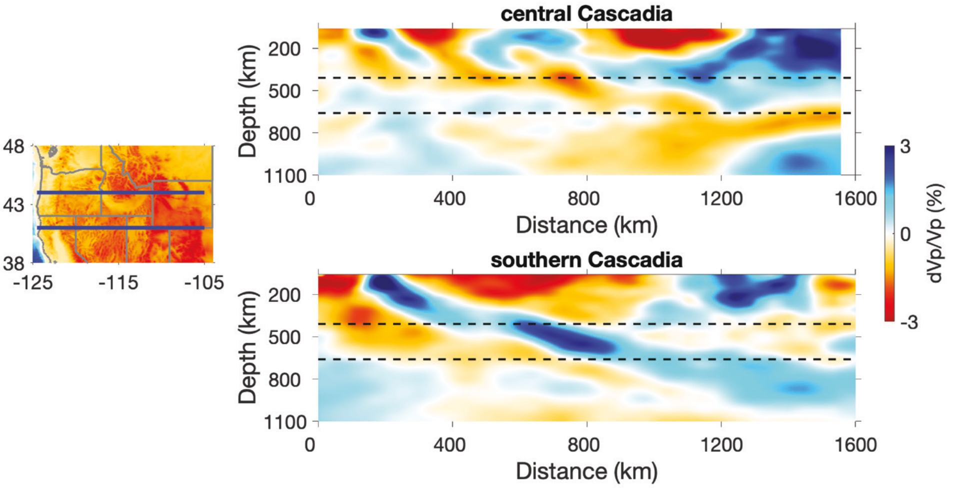

FIGURE 2 West–east vertical profiles of the P-wave velocity perturbations from the velocity model of Schmandt and Lin (2014). The eastward-dipping high-velocity feature is interpreted as the subducting slab. In central Cascadia, the Juan de Fuca slab is imaged at shallow depths. In southern Cascadia, the oceanic slab demonstrates segmentation along the subduction direction.

It is still debated whether the gap revealed by seismic tomographic models corresponds to an actual slab gap or is simply an artifact of the tomographic methods (e.g., Roth et al. 2008; Schmandt and Lin 2014). Furthermore, the subducting slab may be further fragmented at greater depths, as suggested by seismic tomographic models and geodynamic modeling studies (FIG. 2; e.g., Schmandt and Lin 2014; Zhou et al. 2018).

Hydration and Dehydration of the Oceanic Slab

Subduction systems play a key role in the cycling of water and other volatiles between the solid Earth and its outer envelopes. Formed at the mid-ocean ridge, the interior of the oceanic lithosphere is subjected to faulting and deformation as it cools and moves away from the ridge. Hydration of the oceanic lithosphere occurs as a result of hydrothermal circulation near the ridge axis, within the interior of the plate, and near the trench where the plate bends. Bending of the oceanic plate near the trench may reactivate pre-existing faults and/or form new fractures, providing pathways for water to penetrate downward into the oceanic crust and possibly the mantle lithosphere, hydrating it and altering its composition. As the plate subducts, the pressure and temperature increase with depth, resulting in a series of dehydration reactions that progressively release the water bound within the oceanic lithosphere and entrained sediment. The details of water release during the dehydration process—including amounts and locations within the system—play a critical role in controlling wedge rheology, fault behavior at and near the plate interface, and other subduction zone characteristics. In particular, dehydration of the subducting slab triggers partial melting within the mantle wedge and thus volcanism along the arc.

In Cascadia, the young and small JdF oceanic lithosphere leads to a relatively warm and less hydrated subducting slab at the trench. For example, Horning et al. (2016) estimated the amount of water carried within the JdF plate from ridge to trench based on Cascadia active-source seismic experiments. They found that, prior to the subduction of the JdF plate, most water is stored in the oceanic crust and sediments, with very limited water content within the oceanic mantle lithosphere. At the deformation front, most of the water is released and only a small portion of the water is carried deeper down to the mantle wedge. Geophysical studies image low seismic velocities, high electrical conductivity, and distinctive trench-parallel anisotropy in the forearc mantle, suggesting that the forearc region is highly hydrated and serpentinized as a result of shallow slab dehydration (e.g., van Keken et al. 2011). It is generally thought that the total water content released by the young, small, and warm JdF slab at Cascadia is lower than that released at other older and colder subduction systems (e.g., van Keken et al. 2011).

Mantle Flow Within the Cascadia Subduction System

Understanding the pattern of mantle flow in subduction systems provides critical insights into subduction phenomena such as the generation and transport of melt and volatiles, as well as slab morphology and behavior. Two large-scale endmember mantle flow patterns have commonly been inferred at global subduction systems (e.g., Long 2016). The simplest one invokes classical two-dimensional mantle flow, with corner flow above the slab within the mantle wedge and entrained flow beneath the slab. The other endmember model is a complex three-dimensional mantle flow scenario induced by slab rollback; this model invokes the presence of toroidal flow around the edges of the subducting slab, with a significant trench-parallel component. Observations of seismic anisotropy (the dependency of seismic wave speeds on the wave propagation direction) provide a relatively direct way to measure mantle flow patterns. Denser deployment of geophysical instrumentation in the study region allows the mantle flow pattern to be better resolved.

Interestingly, both large-scale endmembers of the mantle flow patterns described above have been invoked in Cascadia (Long 2016). Specifically, seismic anisotropy

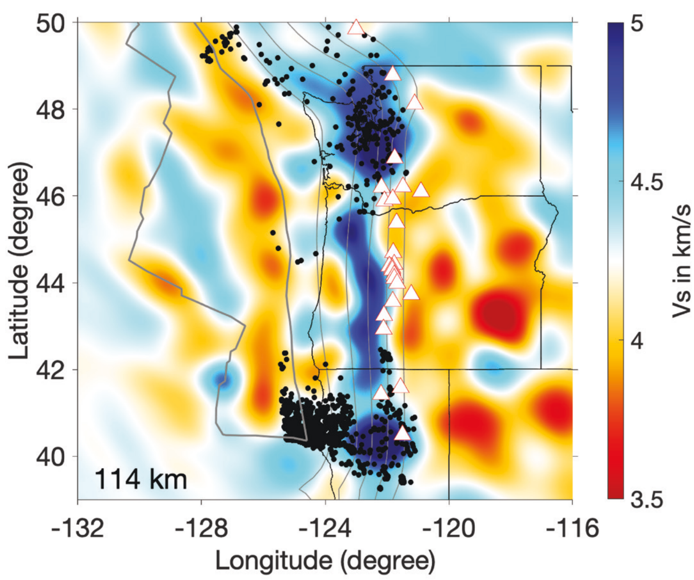

FIGURE 3 Seismic velocity model for the Cascadia subduction system at a depth of 114 km, demonstrating variations in the subducting slab along the trench direction. The Juan de Fuca slab is imaged seismically as a high-velocity feature trending in the south–north direction. The black dots indicate the background seismicity. The triangles represent the Holocene volcanoes. REPRODUCED FROM GAO (2018) WITH PERMISSION FROM NATURE PORTFOLIO.

analyses of Cascadia Initiative data demonstrated that mantle shearing driven by the motion of the JdF plate toward the trench is dominant on the oceanic side prior to subduction (Fig. 4; Bodmer et al. 2015; Martin-Short et al. 2015). Nearly convergence-parallel fast splitting directions are also observed in the central forearc and arc region (Fig. 4; Becker et al. 2012), consistent with two-dimensional corner flow in the wedge and entrained flow beneath the slab. However, many studies have inferred the presence of a three-dimensional toroidal flow pattern at the southern edge of the Cascadia slab in the vicinity of the Mendocino triple junction (Fig. 4). For example, well-organized mantle flow in an east–west direction has been inferred beneath the central portion of the Cascadia backarc. These observations have been interpreted to suggest toroidal mantle flow driven by ongoing slab rollback and trench migration (Long et al. 2012); however, alternative explanations may exist. While relatively sparse station coverage near the northern edge of the Cascadia slab has hampered detailed mapping of the mantle flow field, trench-parallel mantle flow is suggested there by observed spatial variations in trace element and isotopic ratios along the arc volcanoes (Mullen and Weis 2015), consistent with along-strike transport of material in the wedge. In summary, the mantle flow field in Cascadia is likely complex and controlled by a number of factors, including the motion of the downgoing plate, the rollback of the slab, and other possible effects such as lithospheric extension of the Basin and Range, slab tears or fragmentation in the upper mantle, lithospheric delamination, small-scale mantle convection, and plume–slab interactions.

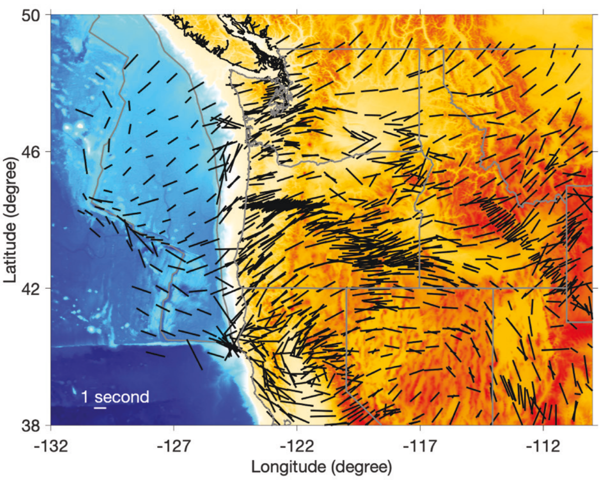

Figure 4 Distribution pattern of seismic anisotropy from the spreading center to the Cascade backarc. The orientations of the bars correspond to the fast-axis direction, and their lengths represent the delay time between the fast and slow shear waves. The shear-wave splitting measurements are from Bodmer et al. (2015) and the compilation of Becker et al. (2012).

Geodynamics of the Cascadia Subduction Zone and Relationships with Melting and Volcanism

One fundamental question is what mechanism controls melt generation in the mantle wedge and the corresponding arc magmatism/volcanism at subduction zones. One commonly invoked mechanism is flux melting in the wedge induced by fluid released from the subducting slab. This mechanism is supported by the hydrous character of arc basalts (e.g., Wiens et al. 2008). Alternatively, decompression melting associated with subduction-induced asthenospheric upwelling from the backarc regions has been proposed to explain the existence of nearly anhydrous (dry) magmatic lavas (e.g., Leeman 2020). Lastly, melting of the oceanic crust and sedimentary layer atop the slab may also contribute and may explain the trace element signatures at some arc volcanoes of global subduction zones (e.g., Wiens et al. 2008).

It is thought that the young and warm JdF plate loses most of its water at shallow depths, leading to less dehydration and smaller water fluxes in the deep crust and upper mantle as the slab descends. Nevertheless, the primitive basalts of the Cascade arc volcanoes show evidence for both wet and dry melting. For example, Mullen et al. (2017) suggest that the compositional variations observed along the Cascade arc are predominantly derived from the slab instead of the mantle wedge. Meanwhile, other studies have observed anhydrous melting in Cascade arc basalts, which has been attributed to subduction-induced decompression melting (Leeman 2020). The seismic velocity model of Gao and Shen (2014) imaged three segmented low-velocity anomalies along the Cascade backarc in the mantle wedge, consistent with the pattern predicted by subduction-induced asthenospheric upwelling that could drive decompression melting. In addition, signatures of melting of the oceanic crust and sedimentary layer atop the slab have also been inferred for Cascade arc magmas (Leeman 2020).

A distinctive aspect of Cascadia is the extensive volcanic and magmatic activity in the backarc region over the last ~17 My. A long-term debate regarding this backarc magmatism is to what extent a mantle plume contributes, as opposed to subduction-related processes. Many studies have proposed that a mantle plume is necessary to explain the eruptive patterns of the Steens/Columbia River basalts and the subsequent formation of the High Lava Plains (HLP) and the Snake River Plain/Yellowstone hotspot track (e.g., Jordan et al. 2004). The presence of a deep mantle plume has been further supported by a recent tomographic model developed by Nelson and Grand (2018), which revealed a low-velocity anomaly extending from the core–mantle boundary to the present-day surface position of the Yellowstone hotspot. However, a variety of non-plume mechanisms have also been proposed that may drive (or at least contribute to) backarc volcanism. For example, rollback and steepening of the subducting slab around 17 Ma may have triggered a pulse of mantle upwelling and melting, with the subsequent evolution of a complex mantle flow field that may have contributed to magmatism in the HLP (Long et al. 2012). In addition, lithospheric extension in the northern Basin and Range may have significantly thinned the continental lithosphere and allowed for asthenospheric upwelling, which may have triggered magmatism in the southern part of the Cascade backarc. Furthermore, localized lithospheric delamination has been proposed beneath northeastern Oregon, and may have contributed to the flood basalt episode (e.g., Hales et al. 2005). It is likely that Cascadia backarc magmatism reflects a combination of slab subduction and rollback, the Yellowstone mantle plume, and lithospheric extension in the Basin and Range.

A number of geodynamic modeling studies have been carried out to investigate mantle flow patterns in Cascadia, relationships between mantle flow and volcanic activity in the backarc, and how a mantle plume may have interacted with the subducting slab. Interestingly, and surprisingly, it appears that both plume models and subduction-driven models (or a combination of these models) can reproduce first-order aspects of backarc magmatism/volcanism. For example, laboratory experiments carried out by Kincaid et al. (2013) demonstrated that a buoyant mantle plume may be divided into two branches by subduction-driven mantle flow, corresponding to the HLP and Snake River Plain/Yellowstone hotspot track. Druken et al. (2011) carried

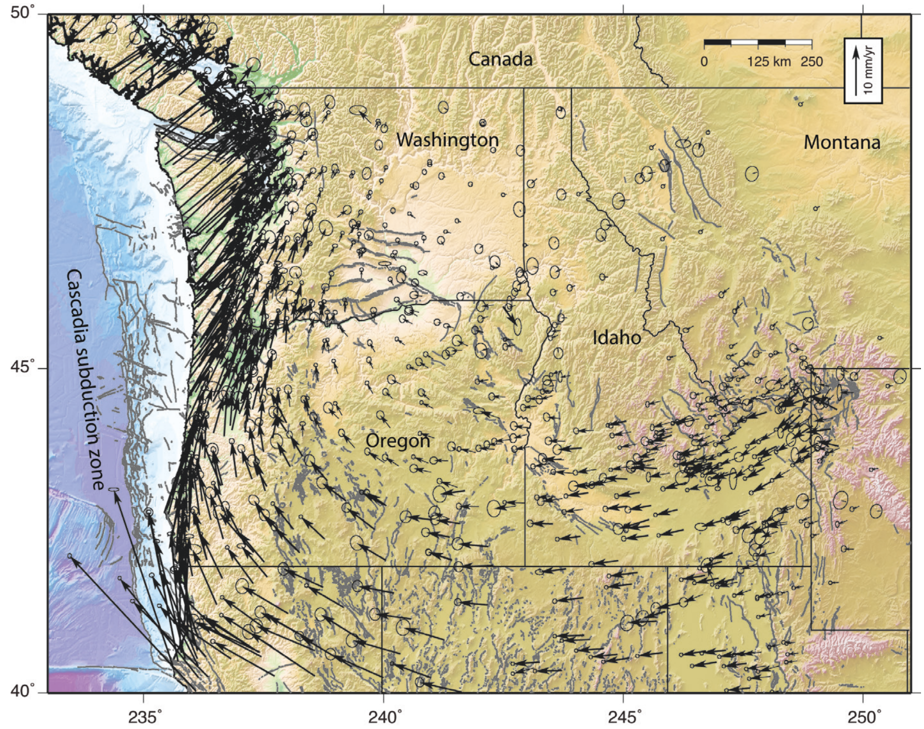

FIGURE 5 Velocity field of the northwestern U.S. relative to North America, inferred from Global Positioning System observations between 1993 and 2011, demonstrating block rotation as well as shortening in the forearc. Error ellipses indicate 70% confidence. REPRODUCED FROM MCCAFFREY ET AL. (2016) WITH PERMISSION FROM OXFORD UNIVERSITY PRESS.

out a series of analog modeling experiments without the presence of a mantle plume and demonstrated that a combination of slab rollback and lithospheric extension well fits the mantle flow pattern observed by seismological studies, as well as the spatiotemporal patterns of HLP volcanism. Liu and Stegman (2012) investigated the relationships between the behavior of the subducting plate and backarc magmatism through a series of numerical models and found that slab tearing can explain the spatial and temporal patterns of the Steens/Columbia River basalt eruptions. Zhou et al. (2018) carried out a series of geodynamic models and demonstrated that observed seismic anisotropy patterns in the western U.S. can be best explained by combined contributions from flow driven by the ongoing subduction of the JdF slab, thickness variations of the continental lithosphere, large-scale mantle flow driven by the deeply subducted Farallon slab beneath the eastern U.S., and the presence of slab tearing.

Crustal Deformation and Kinematics of the Overriding Plate

There are several notable features of Cascadia tectonics that relate to the kinematics of the overriding plate, including extension in the Basin and Range, block rotation of the crust in the backarc, and deformation of the continental crust driven by convergence. While the drivers of Basin and Range extension remain imperfectly understood, a combination of deformation owing to strike-slip motion of the North American and Pacific plates, gravity-driven extension as a result of the thickened crust, and mantle upwelling driven by Farallon/JdF subduction and/or the Yellowstone plume may be responsible (e.g., Camp et al. 2015). Basin and Range extension has progressively migrated northward, reaching its northern and western extent in the Cascade backarc roughly ~5–10 Ma. Extension in the HLP may have been spatially and temporally correlated with backarc volcanism, although the total net extension in this portion of the Cascade backarc has been relatively small compared with the central Basin and Range. The characteristics of the present-day crustal deformation of the overriding plate, illuminated in detail through geodetic measurements (FIG. 5; McCaffrey et al. 2016), include shortening in the Cascade forearc and counter-clockwise block rotation in the central and southern portions of the backarc. Surface velocities derived from geodetic data can also constrain the spatial extent of elastic fault locking at the Cascadia subduction zone megathrust (McCaffrey et al. 2013).

CONCLUDING REMARKS

The Cascadia subduction zone represents a thermally hot endmember of global subduction systems as the oceanic JdF plate is young, warm, and presumably weak. The structure and dynamics of the system have become much better understood over the last decade, in large part because of the increasing availability of geophysical observations. The role of the oceanic lithosphere structure prior to subduction is increasingly recognized as important, a finding enabled by the extensive offshore deployment of geophysical instrumentation. Nevertheless, the precise geometry, characteristics, continuity, and depth extent of the subducting slab remain open questions. Even though numerous geophysical models exist for Cascadia, we still lack a complete and comprehensive model for the structure, kinematics, and dynamics of the entire subduction system, extending from the spreading center to the backarc and from the crust through the mantle lithosphere down to the upper and lower mantle. It appears that subduction-driven processes, including the downdip motion of the plate and slab rollback, exert primary controls on the mantle flow field, which is likely complex and three dimensional, but the details remain to be understood. Key aspects of the

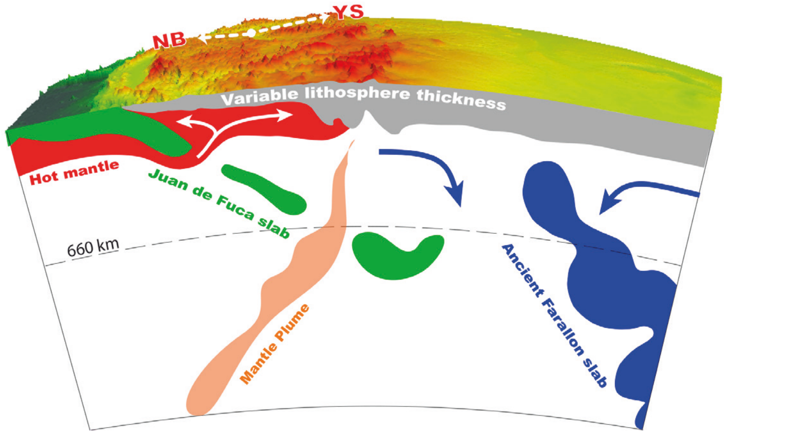

FIGURE 6 Schematic diagram highlighting key dynamic features within the mantle of the U.S., including the young Juan de Fuca slab (green), the old Farallon slab (blue), the possible presence of a deep mantle plume (orange), low-velocity features surrounding the subducting slab (red), and the thickness variation of the continental lithosphere (gray). NB: Newberry Volcano; YS: Yellowstone. REPRODUCED FROM ZHOU ET AL. (2018) WITH PERMISSION FROM ELSEVIER.

subduction system include the linkages among the slab and lithospheric structure, mantle flow, transport and release of water from the subducting slab into the mantle wedge, and magmatic and volcanic expressions at the surface, which are increasingly recognized as important but remain to be explained in detail. It is abundantly clear that there are feedbacks among the fundamental geodynamic processes (Fig. 6) that control the spatial and temporal evolution of arc and backarc magmatism, as well as the tectonic evolution of the overriding plate. Understanding how these processes are linked remains a grand challenge in our study of the Cascadia subduction system.

In the context of this overarching challenge, a number of specific unresolved problems remain. For example, what combination of processes led to the massive flood basalt eruptions approximately 17 Ma? To what extent is a deep mantle plume necessary to explain the magmatic patterns in the Cascade backarc? What is the dominant factor for the observed variations and complexities of the arc volcanoes? What factors control along-strike segmentation in the structure and behavior of the Cascadia subduction zone and its shallow plate interface? What controls the kinematics of the overriding plate, and how do crustal deformation and block rotation affect the subduction system as a whole? Future integrative and multidisciplinary analyses of constraints from geophysics, geochemistry, petrology, geodynamics, geodesy, and structural geology will further our understanding of the Cascadia subduction system.

ACKNOWLEDGMENTS

We thank the guest editors, Adam Kent and Joe Dufek, for their invitation to write this paper. We are grateful to the principal editor Rebecca Lange, guest editor Joe Dufek, and an anonymous reviewer for their thoughtful comments that greatly improved the paper. We thank Lijun Liu and Rob McCaffrey for providing figure files. This work was supported in part by NSF grant EAR-1624077 to H.G.

REFERENCES

Becker TW, Lebedev S, Long MD (2012) On the relationship between azimuthal anisotropy from shear wave splitting and surface wave tomography. Journal of Geophysical Research: Solid Earth 117: B01306, doi: 10.1029/2011JB008705

Bodmer M, Toomey DR, Hooft EE, Nábělek J, Braunmiller J (2015) Seismic anisotropy beneath the Juan de Fuca plate system: evidence for heterogeneous mantle flow. Geology 43: 1095-1098, doi: 10.1130/G37181.1

Bodmer M, Toomey DR, Roering JJ, Karlstrom L (2020) Asthenospheric buoyancy and the origin of high-relief topography along the Cascadia forearc. Earth and Planetary Science Letters 531: 115965, doi: 10.1016/j.epsl.2019.115965

Camp VE, Kenneth LP, Morgan LA (2015) Yellowstone plume trigger for Basin and Range extension, and coeval emplacement of the Nevada–Columbia Basin magmatic belt. Geosphere 11: 203-225, doi: 10.1130/GES01051.1

Druken KA, Long MD, Kincaid C (2011) Patterns in seismic anisotropy driven by rollback subduction beneath the High Lava Plains. Geophysics Research Letters 38: L13310, doi: 10.1029/2011gl047541

Gao H, Humphreys ED, Yao H, van der Hilst RD (2011) Crust and lithosphere structure of the Northwestern U.S. with ambient noise tomography: terrane accretion and Cascade arc development. Earth and Planetary Science Letters 304: 202-211, doi: 10.1016/j.epsl.2011.01.033

Gao H, Shen Y (2014) Upper mantle structure of the Cascades from full-wave ambient noise tomography: evidence for 3D mantle upwelling in the back-arc. Earth and Planetary Science Letters 309: 222-233, doi: 10.1016/j.epsl.2014.01.012

Gao H (2018) Three-dimensional variations of the slab geometry correlate with earthquake distributions at the Cascadia subduction system. Nature Communications 9: 1204, doi: 10.1038/s41467-018-03655-5

Hales TC, Abt DL, Humphreys ED, Roering JJ (2005) A lithospheric instability origin for Columbia River flood basalts and Wallowa mountains uplift in northeast Oregon. Nature 438: 842-845, doi: 10.1038/nature04313

Hawley WB, Allen RM, Richards MA (2016) Tomography reveals buoyant asthenosphere accumulating beneath the Juan de Fuca plate. Science 353: 1406-1408, doi: 10.1126/science.aad8104

Horning G and 5 coauthors (2016) A 2-D tomographic model of the Juan de Fuca plate from accretion at axial seamount to subduction at the Cascadia margin from an active source ocean bottom seismometer survey. Journal of Geophysical Research: Solid Earth 121: 5859-5879, doi: 10.1002/2016JB013228

Jordan BT, Grunder AL, Duncan RA, Deino AL (2004) Geochronology of age-progressive volcanism of the Oregon High Lava Plains: implications for the plume interpretation of Yellowstone. Journal of Geophysical Research: Solid Earth 109, B10202, doi: 10.1029/2003JB002776

Kincaid C, Druken KA, Griffiths RW, Stegman DR (2013) Bifurcation of the Yellowstone plume driven by subduction-induced mantle flow. Nature Geoscience 6: 395-399, doi: 10.1038/ngeo1774

Leeman WP (2020) Old/new subduction zone paradigms as seen from the Cascades. Frontiers in Earth Science 8: 535879, doi: 10.3389/feart.2020.535879

Liu L, Stegman DR (2012) Origin of Columbia River flood basalt controlled by propagating rupture of the Farallon slab. Nature 482: 386-389, doi: http://doi.org/10.1038/nature10749

Long MD and 9 coauthors (2012) Mantle dynamics beneath the Pacific Northwest and the generation of voluminous back-arc volcanism. Geochemistry, Geophysics, Geosystems 13, Q0AN01, doi: 10.1029/2012GC004189

Long MD (2016) The Cascadia paradox: mantle flow and slab fragmentation in the Cascadia subduction system. Journal of Geodynamics 102: 151-170, doi: 10.1016/j.jog.2016.09.006

Martin-Short R, Allen RM, Bastow ID, Totten E, Richards MA (2015) Mantle flow geometry from ridge to trench beneath the Gorda-Juan de Fuca plate system. Nature Geoscience 8: 965-968, doi: 10.1038/ngeo2569

McCaffrey R, King RW, Payne SJ, Lancaster M (2013) Active tectonics of northwestern U.S. inferred from GPS-derived surface velocities. Journal of Geophysical Research: Solid Earth 118: 709-723, doi: 10.1029/2012JB009473

McCaffrey R, King RW, Wells RE, Lancaster M, Miller MM (2016) Contemporary deformation in the Yakima fold and thrust belt estimated with GPS. Geophysical Journal International 207: 1-11, 10.1093/gji/ggw252

Mullen EK, Weis D (2015) Evidence for trench-parallel mantle flow in the northern Cascade arc from basalt geochemistry. Earth and Planetary Science Letters 414: 100-107, doi: 10.1016/j.epsl.2015.01.010

Mullen EK, Weis D, Marsh NB, Martindale M (2017) Primitive arc magma diversity: new geochemical insights in the Cascade arc. Chemical Geology 448: 43-70, doi: 10.1016/j.chemgeo.2016.11.006

Nelson PL, Grand SP (2018) Lower-mantle plume beneath the Yellowstone hotspot revealed by core waves. Nature Geoscience 11: 280-284, doi: 10.1038/s41561-018-0075-y

Roth JB, Fouch MJ, James DE, Carlson RW (2008) Three-dimensional seismic velocity structure of the northwestern United States. Geophysics Research Letters 35: L15304, doi: 10.1029/2008GL034669

Schmandt B, Humphreys E (2011) Seismically imaged relict slab from the 55 Ma Siletzia accretion to the northwest United States. Geology 39: 175-178, doi: 10.1130/G31558.1

Schmandt B, Lin FC (2014) P and S wave tomography of the mantle beneath the United States. Geophysical Research Letters 41: 6342-6349, doi: 10.1002/2014GL061231

van Keken PE, Hacker BR, Syracuse EM, Abers GA (2011) Subduction factory: 4. Depth-dependent flux of H_2O from subducting slabs worldwide. Journal of Geophysical Research: Solid Earth 116: B01401, doi: 10.1029/2010JB007922

Wiens DA, Conder JA, Faul UH (2008) The seismic structure and dynamics of the mantle wedge. Annual Review of Earth and Planetary Sciences 36: 421-455, doi: 10.1146/annurev.earth.33.092203.122633

Zhou Q and 5 coauthors (2018) Western U.S. seismic anisotropy revealing complex mantle dynamics. Earth and Planetary Science Letters 500: 156-167, doi: 10.1016/j.epsl.2018.08.015 ■